Quaternary International 571 (2021) 73–80

Contents lists available at ScienceDirect

Quaternary International

journal homepage: www.elsevier.com/locate/quaint

Indian summer monsoon variability in northeastern India during the last two millennia

Som Dutt [a,*], Anil K. Gupta [b,1], Hai Cheng [c,d,e], Steven C. Clemens [f], Raj K. Singh [g], Vinod C. Tewari [h]

[a] Wadia Institute of Himalayan Geology, 33, General Mahadeo Singh Road, Dehradun, 248001, India
[b] Department of Geology and Geophysics, Indian Institute of Technology Kharagpur, Kharagpur, 721 302, India
[c] Institute of Global Environmental Change, Xi'an Jiaotong University, Xi'an, 710054, China
[d] State Key Laboratory of Loess and Quaternary Geology, Institute of Earth Environment, Chinese Academy of Sciences, Xi'an, 710061, China
[e] Key Laboratory of Karst Dynamics, MLR, Institute of Karst Geology, CAGS, Guilin, 541004, China
[f] Department of Earth, Environmental and Planetary Sciences, 324 Brook Street, PO Box 1846, Brown University, Providence RI 02912-1846, USA
[g] School of Earth, Ocean and Climate Sciences, Indian Institute of Technology Bhubaneswar, Bhubaneswar, 751007, India
[h] Department of Geology, Sikkim University, Gangtok, 737102, India

ARTICLE INFO

Keywords:
MCA
LIA
Last millennium
Late holocene
Indian subcontinent
Speleothems

ABSTRACT

High-resolution proxy records help to understand natural forcing of climate variability and improving our capability to predict climate variability on decadal to centennial time scales. Present study from the Mawmluh cave, northeastern India shows sudden shifts in speleothem oxygen isotope values, indicating several abrupt changes in the Indian summer monsoon (ISM) during ~212 BCE to 1986 CE. Moderate ISM conditions prevailed during ~212 BCE to 400 CE punctuated with weak intervals, strong ISM during 400 and 500 CE and from 640 to 1060 CE, whereas weak ISM conditions prevailed during 520–540 CE, 820–850 CE and 940–980 CE and after 1060 CE. The interval from 1060 to 1986 CE witnessed decreased precipitation than the previous millennium. The latter phase of the Medieval Climate Anomaly (MCA; 1060 to 1200 CE) was quite drier in contrast to the earlier intervals. The ISM was generally weak during the Little Ice Age (LIA; 1350 to 1850 CE) with short-term pulses of high precipitation when sun-spot activity was high. The data shows the weakest ISM condition during 1640–1740 CE (Maunder Minimum) of the last two millennia. Variations in extra-tropical northern hemisphere temperatures due to volcanic activity and solar insolation, and accompanying northward/southward shifting of the Inter-Tropical Convergence Zone played a pivotal role in modulating the strength of the ISM during the past two millennia.

1. Introduction

The last two millennia have been crucial concerning the climate-human interaction, witnessing a sequential rise of human interference in Earth's climate (IPCC, 2013). Several studies indicate a rapid rise in global temperature after the mid-nineteenth century as a result of natural climate cycle as well as enhanced industrial and other developmental activities and forest clearing, etc. (Thompson et al., 2000; Mann and Jones, 2003; Mann et al., 2009). This rapid rise in the global temperature with increased greenhouse gases in atmosphere has had profound effects on global climate leading to increase in the frequency and intensity of extreme events, e.g. increased environmental droughts, more frequent and intense heat waves in Europe and north America, rise in forest fire activity in boreal forests, etc., which can get further intensified in near future (Meehl and Tebaldi, 2004; Kelly et al., 2013; Feurdean et al., 2020; Vicente-Serrano et al., 2020) Both observational and model studies suggest an intensification of monsoon systems including the Indian summer monsoon (ISM) with the increased global warming implying risk of more frequent precipitation extremes (IPCC, 2013; Kitoh et al., 2013; Marcott et al., 2013; Gupta et al., 2019). The risk of more frequent flash floods in the higher reaches is also suggested because of enhanced precipitation in the form of rain (Kitoh et al.,

* Corresponding author.
E-mail addresses: somduttmudgil1@gmail.com, somdutt@wihg.res.in (S. Dutt), anilg@gg.iitkgp.ac.in (A.K. Gupta), cheng021@xjtu.edu.cn (H. Cheng), steven_clemens@brown.edu (S.C. Clemens), rksingh@iitbbs.ac.in (R.K. Singh), vctewari@cus.ac.in (V.C. Tewari).
[1] Formerly at Wadia Institute of Himalayan Geology, Dehradun.

https://doi.org/10.1016/j.quaint.2020.10.021
Received 16 June 2020; Received in revised form 8 October 2020; Accepted 8 October 2020
Available online 14 October 2020

2013).

Such predictive and future projection studies are possible with good understandings of natural processes, occurrence and frequency of climatic events in the past and forcing mechanisms. Availability of long term observational data and high resolution paleoclimate records in Europe and America have imparted confidence for such kind of future climate projections. But such studies are lacking in other parts of the world due to non-availability of long-term meteorological data.

The ISM has crucial importance for survival and socio-economic growth of one third of world's population living in the Indian subcontinent. Any major change in the monsoon behaviour is likely to adversely affect not only the agriculture-based regional economies but global community as is evident from the paleo records of the last few millennia (Yadava et al., 2016; Kathayat et al., 2017; Dutt et al., 2018, 2019). In past few decades, the occurrence of floods have become frequent in India with more intense rains in short intervals and long durations of non rainy seasons due to rising atmospheric temperature and enhanced convective activities (Anderson et al., 2002; Goswami et al., 2006; Singh et al., 2014). Another study suggests a weakening of the south Asian monsoon in some parts of India during the last century due to decrease in land-sea thermal contrast between the Indian Ocean and Indian landmass with warming of the Indian Ocean (Roxy et al., 2015). Therefore there is a need to understand the ISM behaviour in different regions regarding the changing climatic scenario. High-resolution paleoclimatic records indicating the impacts of short-term forcing mechanisms on ISM variability are sparse from the South Asian region. The instrumental records of last one and half century show quasi-oscillatory multi-decadal ISM variability (Krishnamurthy et al., 2000; Goswami et al., 2006), however the number of data sets are not enough to characterise multi-decadal to centennial scale variability in the ISM record. The simulated modelling study suggests that the anthropogenic aerosol loading over southeast Asia has caused summer time drying (Bollsina et al., 2011) but has large uncertainty in the role of aerosol (Gautam et al., 2019). Further, Sinha et al. (2015) have suggested that it is difficult to ascertain the role of anthropogenically forced changes against multi-decadal to centennial-scale natural variability. Hence it is important to assess natural ISM variability in high resolution records from the Indian sub-continent over the last two millennia and forcing mechanisms. To determine changes in the ISM precipitation and the forcing factors which impacted the ISM strength in the last two millennia, we have produced cave carbonate $\delta^{18}O$ record from the Mawmluh cave (25°15′44″N; 91°52′54″E; altitude 1290 m), which is located near Cherrapunji, Meghalaya, northeastern India spanning in age from ~212 BCE to 1986 CE with age uncertainties (Fig. 1). The study region presently receives most of its annual precipitation (~75%) during the summer monsoon season (June to September) through the ISM having its source in the Arabian Sea as well as the Bay of Bengal (Parthasarathy, 1960; Murata et al., 2007; Breitenbach et al., 2010, 2015). The speleothems (cave carbonates) from Meghalaya are one of the best and widely analyzed climate proxies to track changes in the ISM strength on sub-decadal to centennial time scales (Sinha et al., 2011; Berkelhammer et al., 2012; Dutt et al., 2015; Myers et al., 2015; Kathayat et al., 2018; Kaushal et al., 2018). Earlier speleothem studies from this region suggested a strong ISM during the Bølling-Allerød period, early Holocene and late marine isotope stage 3 (Dutt et al., 2015; Lechleitner et al., 2017a). In contrast, weak ISM conditions were observed during the Henrich events, Last Glacial Maximum (LGM), and the Younger Dryas (YD) and 4.2 ka cold events (Berkelhammer et al., 2012; Gupta et al., 2013; Dutt et al., 2015; Lechleitner et al., 2017a; Kathayat et al., 2018).

2. Material and methods

A 23 cm long stalagmite sample MU-1 was collected from the Mawmluh cave, ~4 km inside the cave entrance from a poorly ventilated chamber having stable temperature and more than 95 percent relative humidity. In the laboratory, the stalagmite sample was cut into two halves longitudinally and polished on cut surfaces. The subsamples for various analysis were then extracted along the central growth axis.

The chronology was constrained using eight absolute U–Th series dates determined using the technique as described by Cheng et al. (2013). Each subsample of ~100 mg weight was extracted parallel to the growth of layers. The subsamples were treated with 7 N HNO_3 and then spiked with the known amount of ^{236}U, ^{233}U and ^{229}Th spikes for the accurate measurements of U and Th concentrations and isotopes (Kathayat et al., 2017). U and Th fractions were separated and purified with column chromatography (Edwards et al., 1987). The isotopic compositions of U and Th were analyzed using Thermo Finnigan 'Neptune' multi-collector inductively coupled plasma mass spectrometry (MC-ICPMS) at Xi'an Jiaotong University, China. As the stalagmite

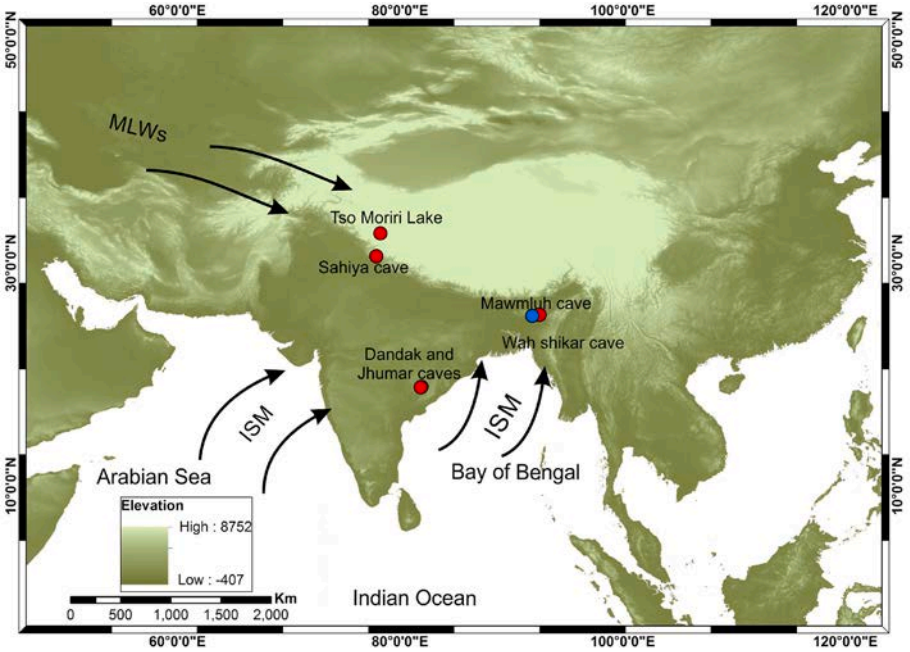

Fig. 1. Location of the Mawmluh cave (blue circle), Meghalaya, northeastern India. Also shown are location of other cave and lake records (red circles) from India whose data has been compared with that from the Mawmluh cave (MU-1). Curved arrows from the Arabian sea and Bay of Bengal show two branches of the Indian summer monsoon (ISM), i.e. Arabian sea branch and Bay of Bengal branch. MLWs represent mid latitude westerlies. (For interpretation of the references to colour in this figure legend, the reader is referred to the Web version of this article.)

was growing and drip water was active at the time of sample collection, the time of stalagmite collection (2009 CE) has been considered as the top age of the sample and used in the age modelling. The age model was initially established using the StalAge program (Scholz and Hoffmann, 2011) in statistical software R (R Development Core Team, 2010). However, considering high age uncertainty, the age model was recalculated using "intra-site correlation age modelling" proposed by Fohlmeister (2012). The published record from the nearby Wah Shikar cave (Sinha et al., 2011; Gupta et al., 2019) were considered for the intra-site correlation and age modelling.

A total of 454 subsamples were extracted for $\delta^{18}O$ measurements at 1 mm interval for the top 3 mm and at every 0.5 mm increment for the rest of the sample. Samples were extracted using a handheld drill, Marathon 3 champion having burs of 0.3 mm diameter. The $\delta^{18}O$ measurements were carried out at Brown University, USA using MAT 252 stable isotope ratio mass spectrometer equipped with a Kiel carbonate III system. The in-house standards of Carrara marble (CM) (n = 58) and Blue Yale marble (BYM) (n = 31) were analyzed repeatedly during the analysis. Replicate analyses of CM and BYM show a precision (1s) of 0.05 and 0.06‰, respectively for oxygen isotopes and 0.02‰ for carbon isotopes during the measurements. The results are reported relative to the VPDB standard in standard delta (δ) notation.

Spectral analysis of the oxygen isotope time series was carried out at 95% confidence level in PAST software using Red Fit and Monte Carlo methods with oversample 1 and number of segments 1 in Blackmann-Harris window (Hammer et al., 2001).

3. Results and proxy interpretation

Results of the age measurements for MU-1 are given in Table 1. The age model suggests a continuous growth of stalagmite MU-1 between 212 BCE and 2009 CE without any hiatus. (Fig. 2). Our record from the Mawmluh cave has an average age uncertainty of ~100 yrs. Such a large age error may not allow to reveal any hiatus of decadal or lower time scale during the deposition. However, northeastern India is one of the highest rainfall regions on earth, and any cessation in stalagmite growth due to no rainfall is very unlikely during the past two millennia, although it may reduce significantly at times. Further, the composite record also does not show any sign of hiatus until 1120 CE and help in

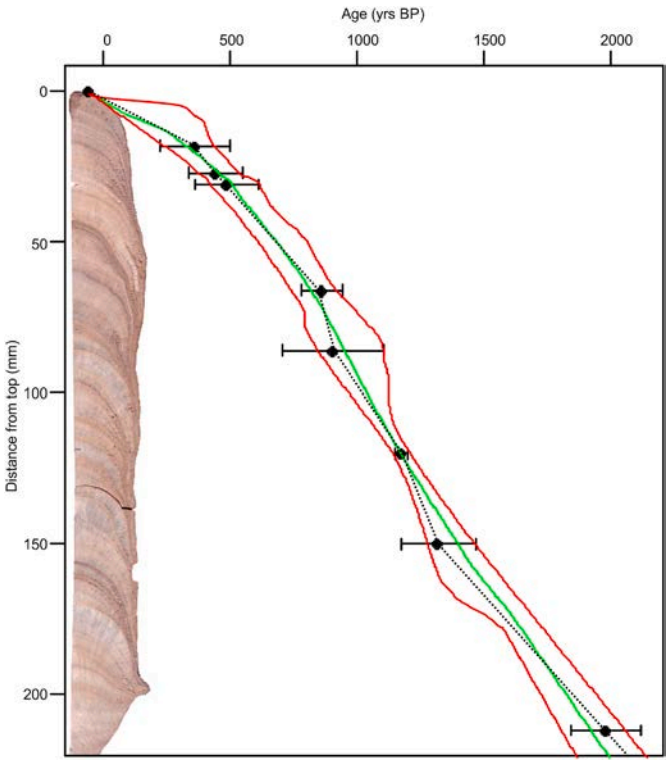

Fig. 2. ^{230}Th age-depth relationship and the age model of MU-1 stalagmite. The age model and corresponding 95% confidence limits are calculated by a Monte Carlo simulation fitting ensembles of red line to subsets of the age data. The age model is established by using ^{230}Th dates (Table 1) and StalAge program in R software. The vertical error bars depict ^{230}Th dating errors (2σ). Green line shows age-depth relation drawn by the StalAge programme. The dotted black line is age-depth relation after making the composite $\delta^{18}O$ time series for northeastern India and used for plotting the MU-1 time series in this study. An image of the stalagmite MU-1 is also shown. (For interpretation of the references to colour in this figure legend, the reader is referred to the Web version of this article.)

Table 1
^{230}Th dating results of stalagmite MU-1 from the Mawmluh cave, northeastern India. The ages are reported in yr BP = years before the Present (A.D. 1950) with 2σ uncertainty. The method is based on Cheng et al. (2013).

Sample Number	Depth (mm)	^{238}U (ppb)	^{232}Th (ppt)	$^{230}Th/^{232}Th$ (atomic $\times10^{-6}$)	$\delta^{234}U$* (measured)	$^{230}Th/^{238}U$ (activity)	^{230}Th Age (yr) (uncorrected)	^{230}Th Age (yr) (corrected)	$\delta^{234}U_{Initial}$** (corrected)	^{230}Th Age (yr BP)*** (corrected)
MU1-1	18 ± 1	6179 ± 12	68140 ± 1370	14 ± 1	664.0 ± 2.4	0.0094 ± 0.0001	620 ± 8	427 ± 137	665 ± 2	364 ± 137
MU1-2	27 ± 1	5571 ± 13	48206 ± 971	19 ± 1	669.2 ± 2.7	0.0101 ± 0.0002	659 ± 10	508 ± 107	670 ± 3	445 ± 107
MU1-7	31 ± 1	5717 ± 39	59257 ± 1237	18 ± 1	711 ± 8	0.0113 ± 0.0002	723 ± 10	547 ± 125	712 ± 9	485 ± 125
MU1-3	66 ± 1	3649 ± 10	22831 ± 461	39 ± 1	572.6 ± 3.1	0.0150 ± 0.0002	1041 ± 14	925 ± 83	574 ± 3	862 ± 83
MU1-4	86 ± 1	3856 ± 11	58075 ± 1173	20 ± 1	563.6 ± 3.3	0.0178 ± 0.0002	1249 ± 14	969 ± 199	565 ± 3	906 ± 199
MU1-8	120 ± 1	6128 ± 33	10418 ± 214	185 ± 4	648 ± 6	0.0191 ± 0.0002	1270 ± 12	1240 ± 25	651 ± 6	1178 ± 25
MU1-5	150 ± 1	5876 ± 15	69199 ± 1397	33 ± 1	639.1 ± 3.0	0.0238 ± 0.0002	1593 ± 11	1384 ± 148	642 ± 3	1321 ± 148
MU1-6	212 ± 1	4525 ± 15	51983 ± 1053	50 ± 1	718.4 ± 3.5	0.0350 ± 0.0002	2238 ± 16	2044 ± 138	723 ± 4	1981 ± 138

U decay constants: $\lambda_{238} = 1.55125 \times 10^{-10}$ (Jaffey et al., 1971) and $\lambda_{234} = 2.82206 \times 10^{-6}$ (Cheng et al., 2013). Th decay constant: $\lambda230 = 9.1705 \times 10^{-6}$ (Cheng et al., 2013).
*$\delta^{234}U$ = ([234U/238U]activity – 1)×1000. **δ^{234}Uinitial was calculated based on 230Th age (T), i.e., δ234Uinitial = δ234Umeasured x eλ234xT.
Corrected ^{230}Th ages assume the initial $^{230}Th/^{232}Th$ atomic ratio of $4.4 \pm 2.2 \times 10^{-6}$. Those are the values for a material at secular equilibrium, with the bulk earth $^{232}Th/^{238}U$ value of 3.8. The errors are arbitrarily assumed to be 50%.
***B.P. stands for "Before Present" where the "Present" is defined as the year 1950 A.D.

minimizing the age uncertainty of MU-1 record. Although some probability of non-deposition due to factors other than rainfall always exists. The average sampling resolution is ~4.8 yr per sample.

The $\delta^{18}O$ ratio from sample MU-1 varies from −6.33 to −2.55‰ with a mean value of −4.1‰ (Fig. 3b). Three different phases are observed in the $\delta^{18}O$ time series of the Mawmluh cave, (i) the highly variable $\delta^{18}O$ ratio has been observed between 212 BCE and ~400 CE but remained close to the mean value except for an interval of much depleted $\delta^{18}O$ values centred at ~130 BCE and highly enriched values during 20–60 CE and slightly enriched during 240–330 and 360–380 CE. The pre and post changes to 20–60 CE and 360–380 CE events are abrupt (Fig. 3b). (ii) Between 400 and ~1060 CE, the $\delta^{18}O$ values remained depleted than the mean value most of the times except an abrupt enrichment at ~500 CE, and others during 820–850 CE and 940–980 CE. The abrupt enrichment

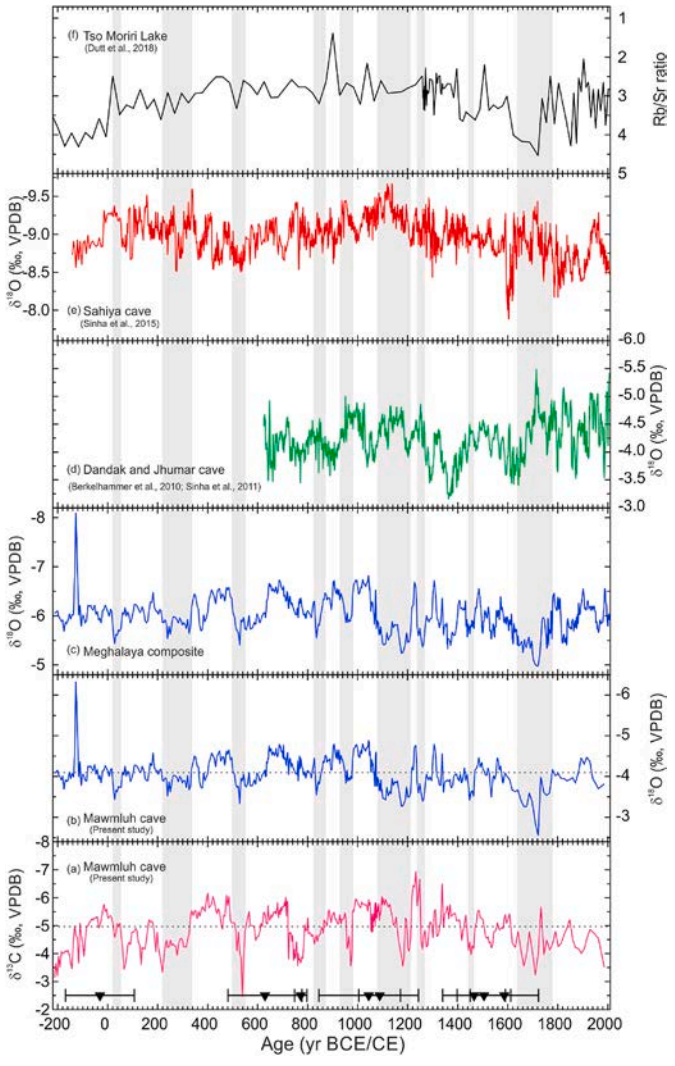

Fig. 3. Indian Summer Monsoon (ISM) proxy record from the Mawmluh cave, Meghalaya, northeastern India compared with other regional paleoclimatic records. (a) $\delta^{13}O$ record for MU-1, Mawmluh cave, northeastern India (this study) for the interval 212 BCE to 1986 CE, (b) $\delta^{18}O$ record of ISM variability from the Mawmluh cave (this study) for the interval 212 BCE to 1986 CE, (c) $\delta^{18}O$ for composite record of Mawmluh and Wah Shikar caves (Sinha et al., 2011 and Gupta et al., 2019) data from Meghalaya, northeastern India, (d) $\delta^{18}O$ record of ISM changes from Dandak and Jhumar caves (Berkelhammer et al., 2010; Sinha et al., 2011), (e) $\delta^{18}O$ record of ISM strength from the Sahiya cave (Sinha et al., 2015), (f) Rb/Sr ratio indicating ISM related changes from the Tso Moriri lake (Dutt et al., 2018). Inverted triagnes in the bottom panel indicate U–Th age measurements of sample MU-1. Grey shaded areas are some of the major weak ISM intervals including the Maunder Minimum.

at ~500 CE centred at around 530 CE shifted towards mean value gradually till ~640 CE. (iii) The $\delta^{18}O$ show a shift towards enriched values after ~1060 CE. The $\delta^{18}O$ values show a general trend of enrichment between 1060 and ~1740 CE with some short spells of lighter values. The most enriched $\delta^{18}O$ values have been observed during ~1640–1740 CE, coinciding with the Maunder Minimum. A trend towards depletion of the $\delta^{18}O$ values is evident after 1740 CE. Due to error in ages, timing of short term climatic events may vary.

The $\delta^{18}O$ ratios in speleothems in northeastern India reflect isotopic signature of the regional precipitation which in itself is influenced by distance travelled by moisture promoting lighter $\delta^{18}O$ at cave site from the farther source due to strong Rayleigh fractionation (Breitenbach et al., 2010), amount of precipitation in large rainstorms giving depletion of $\delta^{18}O$ values (Dansgaard, 1964; Lawrence et al., 2004; Breitenbach et al., 2010), and contribution of isotopically depleted water from freshwater plume in the Bay of Bengal during summer monsoon times (Sengupta and Sarkar, 2006; Singh et al., 2007; Breitenbach et al., 2010). All these processes resulted into depleted $\delta^{18}O$ values in precipitation and cave drip water during and after the ISM season and enriched values during dry season months (Breitenbach et al., 2015a; Myers et al., 2015). The stronger ISM season is characterized by highly negative $\delta^{18}O$ signal, typical to the ISM, in cave drip water and in turn the speleothems deposited at that time (Breitenbach et al., 2015b; Lechleitner et al., 2017a). Therefore, stalagmite $\delta^{18}O$ at Mawmluh cave can be used as a reliable proxy for deducing ISM strength in northeastern India. In this study, more negative $\delta^{18}O$ values of stalagmite have been interpreted as time intervals of strong ISM seasons with higher precipitation in the region and enrichment is suggested as weak ISM accompanying lower rainfall in northeastern India.

The $\delta^{13}C$ values of sample MU-1 are also included in this study. The $\delta^{13}C$ ratios for speleothems reflect changes in the vegetation type (C3 and C4), vegetation intensity, soil processes and kinetic fractionation when combined with the $\delta^{18}O$ values, etc. (Genty et al., 2001; Denniston et al., 2001; Lechleitner et al., 2017a). Changes in vegetation type can be ruled out at quasi sub-decadal scale generally as those changes require longer timescale to change. Vegetation growth above the cave occurs mainly during and post monsoon season due to abundance of water supply, which dissolve $\delta^{13}C$ depleted CO_2 in the percolating water from the soil zone, before dripping in the cave. Observation record from the Mawmluh cave suggests lighter $\delta^{13}C$ values in dripping water during ISM months due to higher vegetation growth above the cave, less ventilation and more close system conditions inside the cave resulting into less degassing from dripping water and less kinetic fractionation (Lechleitner et al., 2017a). In contrary, weak ISM periods witnessed the enriched $\delta^{13}C$ values in cave drip water due to more open system, more ventilation and less vegetation growth above the cave (Lechleitner et al., 2017a). Changes in $\delta^{13}C$ values for MU-1 stalagmite from the Mawmluh cave are more prominent on a short time scale than that of the $\delta^{18}O$ ratio (Fig. 3a). No point to point correlation exists between $\delta^{13}C$ and $\delta^{18}O$ values (R (Anderson et al., 2002) = 0.14) (Fig. 3a and b). The $\delta^{13}C$ values were generally heavier than the mean value between 212 BCE and 330 CE (Fig. 3a). Lighter $\delta^{13}C$ values were observed from 330 to 1400 CE with some multi-decadal scale episodes of enrichment than the mean value, during 720–780CE, 960–980 CE, 1160–1220 CE and maximum enriched value occurred at about 540 CE (Fig. 3a). A long-term trend towards the enrichment of $\delta^{13}C$ values is visible after 1400 CE till 1986 CE.

4. Discussion

The $\delta^{18}O$ record from the Mawmluh cave suggests a significant variability in summer monsoon behaviour during ~212 BCE to 1986 CE (Fig. 3b). Present record suggests moderate summer monsoon conditions prevailed in northeastern India between ~212 BCE and ~400 CE interrupted by weak ISM phases during 20–60 CE, 240–330 and 360–380 CE (Fig. 3b). A long term trend for increasing precipitation is

observed during that period (Fig. 3b). An event of very strong summer monsoon conditions was observed at ~130 BCE (Fig. 3b). Enriched $\delta^{13}C$ values suggest pronounced changes in vegetation growth over the Mawmluh cave (Fig. 3a). This indicates less vegetation growth and more open ventilation in the cave system, indicating less precipitation conditions in northeastern India during 212 BCE to 330 CE (Fig. 3a). From ~212 BCE and ~400 CE, our record suggest moderate to weak ISM conditions in northeastern India, whereas strong ISM conditions were observed in other parts of the Indian subcontinent as indicated by proxy records from Sahiya cave (Fig. 3e), Tso Moriri lake (Fig. 3f), Rewalsar lake (Sinha et al., 2015; Dutt et al., 2018; Singh et al., 2020), and increased *Globigerina bulloides* abundances in the northwestern Arabian Sea indicating an enhanced intensity of summer monsoon winds (Gupta et al., 2003). Proxy record from the Dongge cave also suggests increased monsoonal precipitation during 212 BCE to 400 CE (Wang et al., 2005). This interval is also synchronous with high solar irradiance accompanying high atmospheric temperature in the northern hemisphere (NH) (PAGES 2k, 2013), and northward migration of the Inter Tropical Convergence Zone (ITCZ) (Haug et al., 2001) (Fig. 4). The northward migration of the ITCZ allows movement of strong winds from the Indian Ocean and higher precipitation in the continental interiors (Fleitmann et al., 2003; Dutt et al., 2018). But the summer monsoon conditions observed in northeastern India were not pronounced like other parts of the Indian sub-continent (Fig. 3).

Strong ISM conditions prevailed in northeastern India between 400 and 1060 CE (Figs. 3 and 4). After ~500 CE, a sudden increase in $\delta^{18}O$ values from −4.66 to −3.33‰ was observed indicating an abrupt weakening of the ISM and marked reduction in regional precipitation with weakest ISM conditions at ~530 CE, which changed to moderate precipitation gradually up to 630 CE (Fig. 3b). A large enrichment in $\delta^{13}C$ values at about the same time also testify a sudden weakening of the ISM resulted into lower vegetation growth above the cave site and higher cave ventilation, etc. (Fig. 3a). A forcing mechanism for this sudden ISM weakening is unclear at this point with no evidence of strong ENSO event, reduction in atmospheric temperature or southward migration/contraction of the ITCZ is as observed in the paleoclimatic proxy records (Haug et al., 2001; Rein et al., 2005; Pages2k, 2013) (Fig. 4). This sudden weakening could be related to reduced atmospheric temperature due to large sulphur loadings in the atmosphere as a result of volcanic eruptions, as suggested by Gupta et al. (2019) for some intervals during the LIA. Plummer et al. (2012) suggest extensive volcanogenic sulphur loading to the atmosphere at about the same time (Fig. 4), which might be linked to this ISM weakening. Neverthless, we have poor age constraints to comment on this potential connection and also there is a lack of evidence. This reduced precipitation phase gradually shifted towards moderate summer monsoon at ~640 CE.

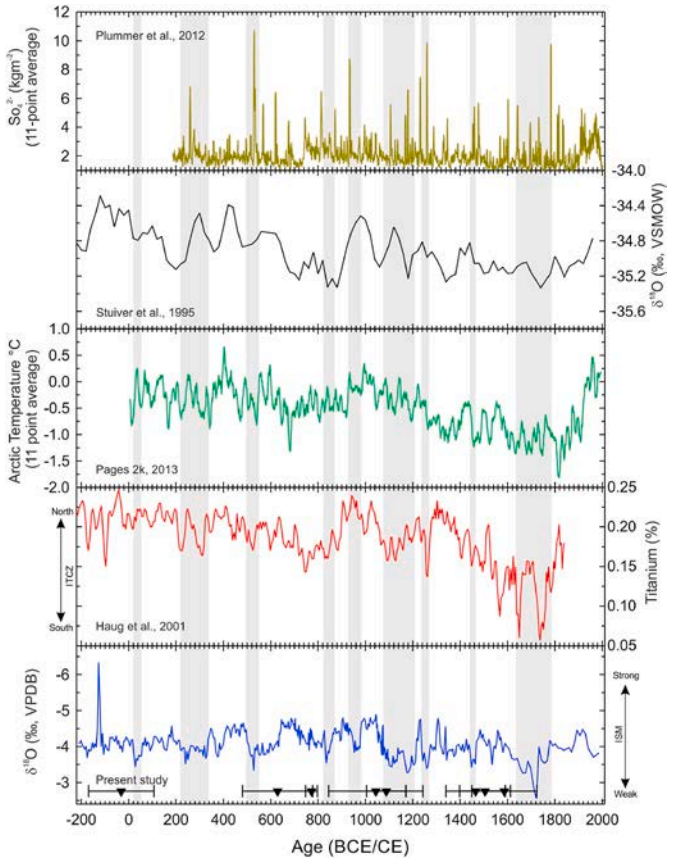

Figure 4. $\delta^{18}O$ record of ISM variability from the Mawmluh cave (this study) for the interval 212 BCE to 1986 CE compared with Ti (%) record of ITCZ migration from ODP Site 1002, Cariaco Basin (Haug et al., 2001), Arctic temperature data, 11 point averaged (PAGES 2k, 2013), $\delta^{18}O$ record from Greenland Ice Sheet Project (GISP) (Stuiver et al., 1995), and Volcanic sulphur loading to the atmosphere, 11-point averaged (Plummer et al., 2012).

Strong ISM conditions between 640 and 1060 CE were interrupted by slightly reduced but moderate precipitation conditions during the eighth and early ninth century CE. Two intervals of slightly below-average precipitation were observed during 820–850 and 940–980 CE. The $\delta^{13}C$ values were also lighter than the mean values during 640–1060 CE and even up to ~1400 CE with multidecadal scale episodes of $\delta^{13}C$ enrichment, prominent at 720-780 , 960–980 and 1160–1220 CE. The period between 640 and 1060 roughly corresponds to the Medieval Climate Anomaly (MCA). Several proxy records suggest a general strong ISM condition during the MCA in the Indian sub-continent (Berkelhammer et al., 2010; Singh et al., 2015; Sinha et al., 2015; Banerji et al., 2020). The westerlies dominated regions of the western Himalaya though represent a dry phase during the MCA (Sharma et al., 2020). The strong monsoon phase between 640 and 1060 CE is linked to high solar insolation, increased temperature in the northern hemisphere and associated northward shifting of the ITCZ (Stuiver et al., 1995; Haug et al., 2001; Tan et al., 2003; Anderson et al., 2004; Pages 2k, 2013) (Fig. 4). During the eighth and ninth centuries CE moderate precipitation conditions, the ITCZ showed a slight southward shift contemporaneous with the cooling in the Arctic and North Atlantic (Fig. 4, Stuiver et al., 1995; Anderson et al., 2004; Pages 2k, 2013), suggesting their role in driving monsoon variability at centennial time scale. The influence of the North Atlantic cooling and NH temperature variability on global climate conditions had earlier been established during the Younger Dryas and Henrich events (Gupta et al., 2003; Broccoli et al., 2006; Jo et al., 2014; Dutt et al., 2015).

Gradual enrichment in $\delta^{18}O$ values suggests decreasing precipitation and weak ISM conditions after 1060, until 1740 CE (Fig. 3b). A delayed enrichment trend in the $\delta^{13}C$ values (Fig. 3a) indicates that the surface vegetation related changes required longer time intervals to respond (Fig. 3a and b). The extra-tropical northern hemisphere also witnessed a decrease in temperature after 10th century CE indicating colder conditions during 1000–1800 CE than the previous millennium (Moberg et al., 2005; Mann et al., 2008; Ljungqvist, 2010). It suggests a close relationship between ISM strength in northeastern India and extra-tropical NH temperatures on multi-centennial to millennial-scale. Long-term global cooling caused the Arctic cooling, increased sea ice in the North Atlantic, weakened Atlantic meridional overturning circulation and southward shift of the ITCZ (Lechleitner et al., 2017b). Our record indicates a dry phase during ~1060–1200 CE, the latter phase of the MCA (Fig. 3b) which has, otherwise, generally been observed as a wet phase in South Asia (Anderson et al., 2002; Wang et al., 2005; Sinha et al., 2011; Sinha et al., 2015). But the timing of the duration of the MCA is highly debatable. Some records also suggest a significant cooling in the 11th century CE ascribed to the Oort solar minimum (Lechleitner et al., 2017b). The decreased global temperature pushed the ITCZ southward and decreased the ISM precipitation in northeastern India. A

record from the Tso Moriri lake suggests a long term decline in ISM precipitation after 1000 CE (Dutt et al., 2018). An age uncertainty can also be held responsible for recording weak ISM during 1060–1200 CE but a long term decline in precipitation is clearly evident linking to the lowered temperatures in the extratropical NH (Figs. 3 and 4). Regional variability is another important aspect in the precipitation conditions throughout the Indian sub-continent during the past two millennia. The PCA analysis of our Mawmluh cave and reconstructed composite $\delta^{18}O$ record of the region between 620 and 1990 CE at decadal resolution suggest no significant correlation with Sahiya cave and composite Dandak and Jhumar cave $\delta^{18}O$ records (Sinha et al., 2011; 15; Dutt et al., 2018, Fig. 5). Similar observations are available from the recent meteorological precipitation data showing no significant correlation between the northwestern and northeastern parts of India (Parthasarathy et al., 1993). Also, the other major climate events such as 4.2 ka event vary temporally and spatially different regions of the Indian sub-continent. This suggests different local forcing factors driving regionally varied precipitation during the last two millennia as observed in the terrestrial proxies from central and northern India (Mishra et al., 2018).

A highly variable but generally a weak summer monsoon was observed in the younger intervals from 1200 to 1740 CE, the LIA occurred between 1350 and 1740 CE with the weakest phase lasting ~100 years during ~1640 to 1740 CE coinciding with the Maunder Minimum (Figs. 3 and 4). A similar weakening of ISM conditions during the Maunder Minimum is evident from a recent speleothem record from the same region (Gupta et al., 2019) and multiple proxy records from the Tso Moriri Lake (Dutt et al., 2018). The Maunder Minimum (1645–1710 CE) was a period of very low temperature when the sun-spot activity was almost absent (Eddy, 1976; Mann and Jones, 2003). The records from the Sahiya cave, Dongge cave and Ganga basin also witnessed a dry phase during the LIA, but timings vary slightly in paleo-records possibly owing to age uncertainties (Wang et al., 2005; Zhang et al., 2008; Sinha et al., 2011; Sinha et al., 2015; Dutt et al., 2018). Records of wet climate are also present from different parts of the Indian sub-continent due to

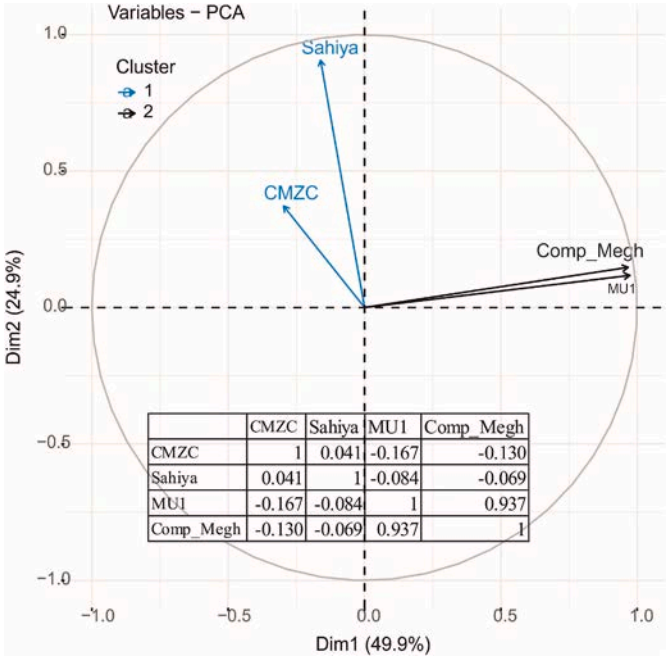

	CMZC	Sahiya	MU1	Comp_Megh
CMZC	1	0.041	-0.167	-0.130
Sahiya	0.041	1	-0.084	-0.069
MU1	-0.167	-0.084	1	0.937
Comp_Megh	-0.130	-0.069	0.937	1

Fig. 5. Principal Component Analysis (PCA) of MU1, Composite Meghalaya (Comp_Megh; comprising of Mawmluh cave and Wah Shikar Cave; Gupta et al., 2019; Sinha et al., 2011), Combined Jhumar and Dandak (CMZC; Sinha et al., 2011) and Sahiya Cave (Kathayat et al., 2018) $\delta^{18}O$ record. Table within the figure are correlation among these data. PCA biplot are grouped by K-means clustering using FactoMiner package in statistical software R (R core team, 2019; Lê et al., 2008).

enhanced winter precipitation mostly through mid-latitude westerlies (Rühland et al., 2006; Kotlia et al., 2012; Banerji et al., 2019; Sharma et al., 2020). Following the Maunder Minimum, the ISM regained its strength with enhanced precipitation in northeastern India (Fig. 3). The trend of variations is almost similar in both the Wah Shikar and Mawmluh caves with slight shifting due to age error.

Multiple intervals of weak and strong ISM conditions occurred during the LIA with changing northern hemisphere temperatures. The decrease in precipitation was driven by the southward migration of the ITCZ resulting from reduced atmospheric temperature because of high sulphur loadings due to widespread volcanism and decreased solar activity, in turn decreasing the atmospheric temperature during the LIA (Miller et al., 2012; Plummer et al., 2012; Sigl et al., 2015; Gupta et al., 2019). The weak summer monsoon phases after 1060 CE had profound effects on the socio-economic conditions in South Asia during the last millennium (Yadav et al., 2016; Gupta et al., 2019). Low rainfall largely impacted the agricultural production in the region and in turn, the economy in the Indian sub-continent. The Pala Empire collapsed in Bengal during the 11th century CE and Sena Empire in the 12th century CE (Majumdar et al., 1978). Foreign invasions also became frequent in India from 11th century CE onwards. Collapse of economy due to less rainfall, foreign invasions and plunders, and internal strife for resources led socio-economic conditions and industries in India to very low productivity and led to establishment of foreign rules in India. The large empires with flourishing economies existed during the phases of strong and equable monsoon conditions but fragmented into small states with very frequent clashes for resources during low and highly variable rainfall conditions (Majumdar et al., 1978; Kumar et al., 2013; Gupta et al., 2019). The disintegration of Gupta Empire into several small states during the mid-sixth century CE (Majumdar et al., 1978) might also had some link to the reduced ISM rainfall after 500 CE with very low rainfall during 520–540 CE in addition to the foreign invasions. After 1740 CE, ISM precipitation began to increase with a rise in atmospheric warming due to enhanced sun-spot activity accompanying the anthropogenic factors (Eddy, 1976; Steinhilber et al., 2012; Gupta et al., 2019).

A correlation of our record of ISM strength in northeastern India with the temperature reconstruction from the extratropical NH and latitudinal positioning of the ITCZ indicates a strong linkage of ISM strength with shifts in the ITCZ and Arctic temperature (Fig. 4) (Haug et al., 2001; Mann and Jones, 2003). The periods of high/low temperature in the NH are aligned with intervals of northward/southward migration of the ITCZ and strong/weak summer monsoon conditions in northeastern India (Fig. 4). The strong periodicity of ~315 yr solar cycle, and small 16 and 10 yr cycles (sun-spot cycle) further strengthen our understanding of the sun-monsoon linkages over the Indian sub-continent (Fig. 6; Fleitmann et al., 2003; Wang et al., 2005).

5. Conclusions

Our speleothem record from the Mawmluh cave indicates highly variable Indian summer monsoon (ISM) strength during 212 BCE to 1986 CE. Moderate ISM conditions were observed between ~212 BCE and 400 CE, strong ISM during 400–500 CE and from 640 to 1060 CE, whereas weak ISM conditions prevailed during 520–540 CE, 820–850 CE and 940–980 CE and after 1060 CE. Multiple phases of strong and weak ISM were observed during the Medieval Climate Anomaly and Little Ice Age. ISM precipitation significantly decreased during the 2nd millennium CE from the 1st millennium CE in northeastern India. The weakest phase of the ISM occurred during the Maunder Minimum, following which the ISM has intensified. Changes in high latitude northern hemisphere temperatures and latitudinal position of the ITCZ driven by solar activity and volcanism played a pivotal role in driving ISM variability during the past two millennia.

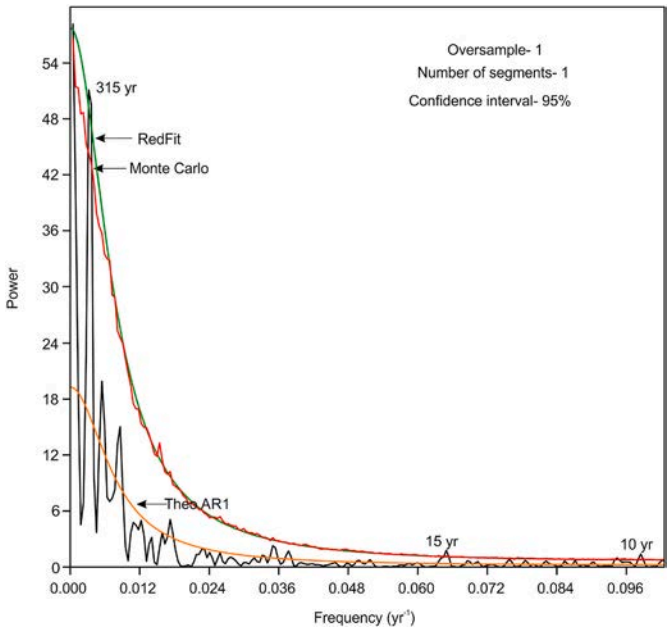

Fig. 6. Spectral analysis of MU-1 $\delta^{18}O$ time series for the period 212BCE to 1986 CE showing statistically most significant periodicities (95%) centred at 315, 15, and 10 yr using PAST RedFit and Monte Carlo methods at Oversample 1 and number of segments 1. Software is available at https://folk.uio.no/ohammer/past/.

Authors contributions

S.D., A.K.G. and R.K.S. interpreted the results and wrote the manuscript. V.C.T. collected the sample and helped in manuscript preparation, R.K.S. extracted sub-samples and did composite and PCA analysis, H.C. helped in Uranium series dating of samples and data interpretation, S.C.C. helped in stable isotope analysis and data interpretation. Correspondence and requests for materials should be addressed to S.D. (somduttmudgil1@gmail.com) and A.K.G. (anilg@gg.iitkgp.ac.in).

Declaration of competing interest

The authors declare that they have no known competing financial interests or personal relationships that could have appeared to influence the work reported in this paper.

Acknowledgements

S.D. thanks the Wadia Institute of Himalayan Geology for providing infrastructure facilities under contribution number WIHG/0105. A.K.G. thanks the Department of Science and Technology, New Delhi for funding under Sir J.C. Bose fellowship (SR/S2/JCB-80/2011). RKS acknowledges IIT Bhubaneswar (SP 053) and MoES, Govt. of India (RP-088) for support. H.C. acknowledges the support from the NSFC (Grant No. 41888101). Wadia Institute of Himalayan Geology provided the infrastructure and basic facilities to carry out this research. Editor and two anonymous reviewers are also thanked for their comments and suggestions that helped in improving the manuscript. Data for this study can be downloaded at https://doi.org/10.17632/58bs5hctxr.3.

References

Andersen, K.K., North Greenland Ice Core Project members, 2004. High-resolution record of Northern Hemisphere climate extending into the last interglacial period. Nature 431 (7005), 147.

Anderson, D.M., Overpeck, J., Gupta, A.K., 2002. Increase in the asian southwest monsoon during the past four centuries. Science 297, 596–599.

Banerji, U.S., Bhushan, R., Jull, A.T., 2019. Signatures of global climatic events and forcing factors for the last two millennia from the active mudflats of Rohisa, southern Saurashtra, Gujarat, western India. Quat. Int. 507, 172–187.

Banerji, U.S., Arulbalaji, P., Padmalal, D., 2020. Holocene climate variability and Indian Summer Monsoon: an overview. Holocene, 0959683619895577.

Berkelhammer, M., Sinha, A., Mudelsee, M., Edwards, R.L., Cannariato, K., 2010. Persistent multidecadal power of the Indian summer monsoon. Earth Planet Sci. Lett. 290, 166–172.

Berkelhammer, M., Sinha, A., Stott, L., Cheng, H., Pausata, F.S., Yoshimura, K., 2012. An abrupt shift in the Indian monsoon 4000 Years ago. In: Giosan, L., et al. (Eds.), Climates, Landscapes, and Civilizations: American Geophysical Monograph, vol. 198, pp. 75–87. https://doi.org/10.1029/2012GM001207.

Breitenbach, S.F.M., Adkins, J.F., Meyer, H., Marwan, N., Kumar, K.K., Haug, G.H., 2010. Strong influence of water vapor source dynamics on stable isotopes in precipitation observed in Southern Meghalaya, NE India. Earth Planet Sci. Lett. 292, 212–220. https://doi.org/10.1016/j.epsl.2010.01.038.

Breitenbach, S.F.M., Lechleitner, F.A., Meyer, H., Diengdoh, G., Mattey, D., Marwan, N., 2015a. Cave ventilation and rainfall signals in dripwater in a monsoonal setting – a monitoring study from NE India. Chem. Geol. 402, 111–124.

Breitenbach, S.F., Lechleitner, F.A., Meyer, H., Diengdoh, G., Mattey, D., Marwan, N., 2015b. Cave ventilation and rainfall signals in dripwater in a monsoonal setting–a monitoring study from NE India. Chem. Geol. 402, 111–124.

Broccoli, A.J., Dahl, K.A., Stouffer, R.J., 2006. Response of the ITCZ to northern hemisphere cooling. Geophys. Res. Lett. 33 (1).

Cheng, H., Edwards, R.L., Shen, C.-C., Polyak, V.J., Asmerom, Y., Woodhead, J., Hellstrom, J., Wang, Y., Kong, X., Spötl, C., Wang, X., 2013. Improvements in ^{230}Th dating, ^{230}Th and ^{234}U half-life values, and U–Th isotopic measurements by multi-collector inductively coupled plasma mass spectrometry. Earth Planet Sci. Lett. 371–372, 82–91. https://doi.org/10.1016/j.epsl.2013.04.006.

Dansgaard, W., 1964. Stable isotopes in precipitation. Tellus 16, 436–468.

Denniston, R.F., Gonzalez, L.A., Asmerom, Y., Polyak, V., Reagan, M.K., Saltzman, M.R., 2001. A high-resolution speleothem record of climatic variability at the Allerød–Younger Dryas transition in Missouri, central United States. Palaeogeogr. Palaeoclimatol. Palaeoecol. 176 (1–4), 147–155.

Dutt, S., Gupta, A.K., Clemens, S.C., Cheng, H., Singh, R.K., Kathayat, G., Edwards, R.L., 2015. Abrupt changes in Indian summer monsoon strength during 33,800 to 5500 years B. P. Geophys. Res. Lett. 42, 5526–5532. https://doi.org/10.1002/2015GL064015.

Dutt, S., Gupta, A.K., Wünnemann, B., Yan, D., 2018. A long arid interlude in the Indian summer monsoon during ~4,350 to 3,450 cal. yr BP contemporaneous to displacement of the Indus valley civilization. Quat. Int. 482, 83–92. https://doi.org/10.1016/j.quaint.2018.04.005.

Dutt, S., Gupta, A.K., Singh, M., Jaglan, S., Saravanan, P., Balachandiran, P., Singh, A., 2019. Climate variability and evolution of the Indus civilization. Quat. Int. 507, 15–23.

Eddy, J.A., 1976. The maunder minimum. Science 192, 1189–1202.

Edwards, R.L., Chen, J.H., Wasserburg, G.J., 1987. ^{238}U-^{234}U-^{230}Th-^{232}Th systematics and the precise measurement of time over the past 500,000 years. Earth Planet Sci. Lett. 81, 175–192.

Feurdean, A., Florescu, G., Tanţău, I., Vannière, B., Diaconu, A.C., Pfeiffer, M., Waren, D., Hutchinson, S.M., Gorina, N., Galka, M., Kirpotin, S., 2020. Recent fire regime in the southern boreal forests of western Siberia is unprecedented in the last five millennia. Quat. Sci. Rev. 244, 106495.

Fleitmann, D., Burns, S.J., Mudelsee, M., Fleitmann, D., Burns, S.J., Mudelsee, M., Neff, U., Kramers, J., Mangini, A., Matter, A., 2003. Holocene forcing of the Indian monsoon recorded in a stalagmite from southern Oman. Science 300, 1737–1739. https://doi.org/10.1126/science.1083130.

Fohlmeister, J., 2012. A statistical approach to construct composite climate records of dated archives. Quat. Geochronol. 14, 48–56.

Genty, D., Baker, A., Massault, M., Proctor, C., Gilmour, M., Pons-Branchu, E., Hamelin, B., 2001. Dead carbon in stalagmites: carbonate bedrock paleodissolution vs. ageing of soil organic matter. Implications for 13C variations in speleothems. Geochem. Cosmochim. Acta 65 (20), 3443–3457.

Goswami, B.N., Venugopal, V., Sengupta, D., Madhusoodanan, M.S., Xavier, P.K., 2006. Increasing trend of extreme rain events over India in a warming environment. Science 314, 1442–1445. https://doi.org/10.1126/science.1132027.

Gupta, A.K., Anderson, D.M., Overpeck, J.T., 2003. Abrupt changes in the asian southwest monsoon during the Holocene and their links to the north atlantic ocean. Nature 421, 354–357. https://doi.org/10.1038/nature01340.

Gupta, A.K., Dutt, S., Cheng, H., Singh, R.K., 2019. Abrupt changes in Indian summer monsoon strength during the last~ 900 years and their linkages to socio-economic conditions in the Indian subcontinent. Palaeogeo.Palaeoclim.Palaeoecol. 536, 109347. https://doi.org/10.1016/j.palaeo.2019.109347.

Hammer, Ø., Harper, D.A.T., Ryan, P.D., 2001. PAST: paleontological statistics software package for education and data analysis. Palaeontol. Electron. 4, 1–9.

Haug, G.H., Hughen, K.A., Sigman, D.M., Peterson, L.C., Röhl, U., 2001. Southward migration of the intertropical convergence zone through the Holocene. Science 293, 1304–1308. https://doi.org/10.1126/science.1059725.

Intergovernmental Panel on Climate Change (IPCC), 2013. Climate change 2013: the physical science basis. In: Stocker, T.F., et al. (Eds.), Contribution of Working Group I to the Fifth Assessment Report of the Intergovernmental Panel on Climate Change. Cambridge University Press, Cambridge, UK, pp. 35–118.

Jo, K.N., Woo, K.S., Yi, S., Yang, D.Y., Lim, H.S., Wang, Y., Cheng, H., Edwards, R.L., 2014. Mid-latitude interhemispheric hydrologic seesaw over the past 550,000 years. Nature 508 (7496), 378.

Kathayat, G., Cheng, H., Sinha, A., Yi, L., Li, X., Zhang, H., Li, H., Ning, Y., Edwards, R.L., 2017. The Indian monsoon variability and civilization changes in the Indian subcontinent. Sci. Adv. 3, e1701296 https://doi.org/10.1126/sciadv.1701296.

Kathayat, G., Cheng, H., Sinha, A., Berkelhammer, M., Zhang, H., Duan, P., Li, H., Li, X., Ning, Y., Edwards, R.L., 2018. Evaluating the timing and structure of the 4.2 ka event in the Indian summer monsoon domain from an annually resolved speleothem record from Northeast India. Clim. Past 14, 1869–1879. https://doi.org/10.5194/cp-14-1869-2018.

Kaushal, N., Breitenbach, S.F.M., Lechleitner, F.A., Sinha, A., Tewari, V.C., Ahmad, S.M., Berkelhammer, M., Band, S., Yadava, M., Ramesh, R., Henderson, G.M., 2018. The Indian summer monsoon from a speleothem $\delta^{18}O$ perspective—a review. Quaternary 1 (3), 29.

Kelly, R., Chipman, M.L., Higuera, P.E., Stefanova, I., Brubaker, L.B., Hu, F.S., 2013. Recent burning of boreal forests exceeds fire regime limits of the past 10,000 years. Proc. .Natl. Sci. Acad. 110 (32), 13055–13060.

Kitoh, A., Endo, H., Krishna Kumar, K., Cavalcanti, I.F., Goswami, P., Zhou, T., 2013. Monsoons in a changing world: a regional perspective in a global context. J. Geophys. Res. Atmos. 118, 3053–3065. https://doi.org/10.1002/jgrd.50258.

Kotlia, B.S., Ahmad, S.M., Zhao, J.X., Raza, W., Collerson, K.D., Joshi, L.M., Sanwal, J., 2012. Climatic fluctuations during the LIA and post-LIA in the Kumaun Lesser Himalaya, India: evidence from a 400 y old stalagmite record. Quat. Int. 263, 129–138.

Kumar, D., Raychaudhuri, T., Habib, I. (Eds.), 2013. The Cambridge Economic History of India, vol. 1. Harrassowitz Verlag, pp. c.1200–c.1750.

Lawrence, J.R., Gedzelman, S.D., Dexheimer, D., Cho, H.K., Carrie, G.D., Gasparini, R., Anderson, C.R., Bowman, K.P., Biggerstaff, M.I., 2004. Stable isotopic composition of water vapor in the tropics. J. Geophys. Res. Atmos. 109, D06115.

Lê, S., Josse, J., Husson, F., 2008. FactoMineR: a package for multivariate analysis. J. Stat. Software 25 (1), 1–18. https://doi.org/10.18637/jss.v025.i01.

Lechleitner, F.A., Breitenbach, S.F., Cheng, H., Plessen, B., Rehfeld, K., Goswami, B., Marwan, N., Eroglu, D., Adkins, J., Haug, G., 2017a. Climatic and in-cave influences on $\delta^{18}O$ and $\delta^{13}C$ in a stalagmite from northeastern India through the last deglaciation. Quat. Res. 88, 458–471. https://doi.org/10.1017/qua.2017.72.

Lechleitner, F.A., Breitenbach, S.F., Rehfeld, K., Ridley, H.E., Asmerom, Y., Prufer, K.M., Marwan, N., Goswami, B., Kennett, D.J., Aquino, V.V., Polyak, V., 2017b. Tropical rainfall over the last two millennia: evidence for a low-latitude hydrologic seesaw. Sci. Rep. 7, 45809.

Ljungqvist, F.C., 2010. A new reconstruction of temperature variability in the extra-tropical Northern Hemisphere during the last two millennia. Geogr. Ann.: Series A Physical Geography 92, 339–351. https://doi.org/10.1111/j.1468-0459.2010.00399.x.

Majumdar, R.C., Raychaudhuri, H., Datta, K., 1978. An Advanced History of India, fourth ed. Macmillan Publishers India Limited, Delhi, India.

Mann, M.E., Jones, P.D., 2003. Global surface temperatures over the past two millennia. Geophys. Res. Lett. 30, 1820. https://doi.org/10.1029/2003GL017814.

Mann, M.E., Zhang, Z., Hughes, M.K., Bradley, R.S., Miller, S.K., Rutherford, S., Ni, F., 2008. Proxy-based reconstructions of hemispheric and global surface temperature variations over the past two millennia. Proc. Natl. Sci. Acad. USA. 105 (36), 13252–13257.

Mann, M.E., Zhang, Z., Rutherford, S., Bradley, R.S., Hughes, M.K., Shindell, D., Ammann, C., Faluvegi, G., Ni, F., 2009. Global signatures and dynamical origins of the Little ice age and medieval climate anomaly. Science 326, 1256–1260. https://doi.org/10.1126/science.1177303.

Marcott, S.A., Shakun, J.D., Clark, P.U., Mix, A.C., 2013. A reconstruction of regional and global temperature for the past 11,300 years. Science 339, 1198–1201. https://doi.org/10.1126/science.1228026.

Meehl, G.A., Tebaldi, C., 2004. More intense, more frequent, and longer lasting heat waves in the 21st century. Science 305 (5686), 994–997.

Miller, G.H., Geirsdóttir, Á., Zhong, Y., Larsen, D.J., Otto-Bliesner, B.L., Holland, M.M., Bailey, D.A., Refsnider, K.A., Lehman, S.J., Southon, J.R., Anderson, C., 2012. Abrupt onset of the Little Ice Age triggered by volcanism and sustained by sea-ice/ocean feedbacks. Geophys. Res. Lett. 39, L02708.

Mishra, P.K., Prasad, S., Marwan, N., Anoop, A., Krishnan, R., Gaye, B., Basavaiah, N., Stebich, M., Menzel, P., Riedel, N., 2018. Contrasting pattern of hydrological changes during the past two millennia from central and northern India: regional climate difference or anthropogenic impact? Global Planet. Change 161, 97–107.

Moberg, A., Sonechkin, D.M., Holmgren, K., Datsenko, N.M., Karlén, W., 2005. Highly variable Northern Hemisphere temperatures reconstructed from low-and high-resolution proxy data. Nature 433 (7026), 613.

Murata, F., Hayashi, T., Matsumoto, J., Asada, H., 2007. Rainfall on the Meghalaya plateau in northeastern India-one of the rainiest places in the world. Nat. Hazards 42, 391–399. https://doi.org/10.1007/s11069-006-9084-z.

Myers, C.G., Oster, J.L., Sharp, W.D., Bennartz, R., Kelley, N.P., Covey, A.K., Breitenbach, S.F.M., 2015. Northeast Indian stalagmite records Pacific decadal climate change: implications for moisture transport and drought in India. Geophys. Res. Lett. 42, 4124–4132. https://doi.org/10.1002/2015GL063826.

PAGES, 2k, 2013. Continental-scale temperature variability during the past two millennia. Nat. Geosci. 6, 339–346. https://doi.org/10.1038/ngeo1797.

Parthasarathy, K., 1960. Some aspects of rainfall in India during the Southwest monsoon season. In: Proceedings of the Symposium on Monsoon of the World. India Meteorological Department, New Delhi, pp. 185–194.

Parthasarathy, B., Kuma, K.R., Munot, A.A., 1993. Homogeneous Indian monsoon rainfall: variability and prediction. Proc. Indian Acad. Sci. Earth Planet Sci. 102, 121–155.

Plummer, C.T., Curran, M.A., van Ommen, T.D., Rasmussen, S.O., Moy, A.D., Vance, T. R., Clausen, H.B., Vinther, B.M., Mayewski, P.A., 2012. An independently dated 2000-yr volcanic record from Law Dome, East Antarctica, including a new perspective on the dating of the 1450s CE eruption of Kuwae. Vanuatu. Clim. Past 8 (6), 1929–1940.

R Development Core Team, 2010. R: A Language and Environment for Statistical Computing. R Foundation for Statistical Computing, Vienna, Austria.

Rein, B., Lückge, A., Reinhardt, L., Sirocko, F., Wolf, A., Dullo, W.C., 2005. El Niño variability off Peru during the last 20,000 years. Paleoceanography 20 (4), PA4003.

Roxy, M.K., Ritika, K., Terray, P., Murtugudde, R., Ashok, K., Goswami, B.N., 2015. Drying of Indian subcontinent by rapid Indian Ocean warming and a weakening land-sea thermal gradient. Nat. Commun. 6, 7423. https://doi.org/10.1038/ncomms8423.

Rühland, K., Phadtare, N.R., Pant, R.K., Sangode, S.J., Smol, J.P., 2006. Accelerated melting of Himalayan snow and ice triggers pronounced changes in a valley peatland from northern India. Geophys. Res. Lett. 33 (15), GL026704.

Scholz, D., Hoffmann, D.L., 2011. StalAge-An algorithm designed for construction of speleothem age models. Quat. Geochronol. 6, 369–382. https://doi.org/10.1016/j.quageo.2011.02.002.

Sengupta, S., Sarkar, A., 2006. Stable isotope evidence of dual (Arabian Sea and Bay of Bengal) vapour sources in monsoonal precipitation over north India. Earth Planet Sci. Lett. 250, 511–521.

Sharma, C.P., Rawat, S.L., Srivastava, P., Meena, N.K., Agnihotri, R., Kumar, A., Chahal, P., Gahlaud, S.K.S., Shukla, U.K., 2020. High-resolution climatic (monsoonal) variability reconstructed from a continuous~ 2700-year sediment record from Northwest Himalaya (Ladakh). Holocene 30 (3), 441–457.

Sigl, M., Winstrup, M., McConnell, J.R., Welten, K.C., Plunkett, G., Ludlow, F., Büntgen, U., Caffee, M., Chellman, N., Dahl-Jensen, D., Fischer, H., 2015. Timing and climate forcing of volcanic eruptions for the past 2,500 years. Nature 523 (7562), 543.

Singh, M., Singh, I.B., Müller, G., 2007. Sediment characteristics and transportation dynamics of the Ganga River. Geomorphology 86, 144–175.

Singh, D., Tsiang, M., Rajaratnam, B., Diffenbaugh, N.S., 2014. Observed changes in extreme wet and dry spells during the South Asian summer monsoon season. Nat. Clim. Change 4 (6), 456–461.

Singh, S., Gupta, A.K., Dutt, S., Bhaumik, A.K., Anderson, D.M., 2020. Abrupt shifts in the Indian summer monsoon during the last three millennia. Quat. Int. 558, 59–65. https://doi.org/10.1016/j.quaint.2020.08.033.

Singh, D.S., Gupta, A.K., Sangode, S.J., Clemens, S.C., Prakasam, M., Srivastava, P., Prajapati, S.K., 2015. Quat. Int. 371, 157–163. https://doi.org/10.1016/j.quaint.2015.02.040.

Sinha, A., Berkelhammer, M., Stott, L., Mudelsee, M., Cheng, H., Biswas, J., 2011. The leading mode of Indian summer monsoon precipitation variability during the last millennium. Geophys. Res. Lett. 38, L15703. https://doi.org/10.1029/2011GL047713.

Sinha, A., Kathayat, G., Cheng, H., Breitenbach, S.F.M., Berkelhammer, M., Mudelsee, M., Biswas, J., Edwards, R.L., 2015. Trends and oscillations in the Indian summer monsoon rainfall over the last two millennia. Nat. Commun. 6, 6309. https://doi.org/10.1038/ncomms7309.

Steinhilber, F., Abreu, J.A., Beer, J., Brunner, I., Christl, M., Fischer, H., Heikkilä, U., Kubik, P.W., Mann, M., McCracken, K.G., Miller, H., 2012. 9,400 years of cosmic radiation and solar activity from ice cores and tree rings. Proc. Natl. Sci. Acad. USA 109 (16), 5967–5971.

Tan, M., Liu, T., Hou, J., Qin, X., Zhang, H., Li, T., 2003. Cyclic rapid warming on centennial-scale revealed by a 2650-year stalagmite record of warm season temperature. Geophys. Res. Lett. 30 (12) https://doi.org/10.1029/2003GL017352, 2003.

Thompson, L.G., Yao, T., Mosley-Thompson, E., Davis, M.E., Henderson, K.A., Lin, P.N., 2000. A high-resolution millennial record of the South Asian monsoon from Himalayan ice cores. Science 289, 1916–1919. https://doi.org/10.1126/science.289.5486.1916.

Vicente-Serrano, S.M., Quiring, S.M., Peña-Gallardo, M., Yuan, S., Domínguez-Castro, F., 2020. A review of environmental droughts: increased risk under global warming? Earth Sci. Rev. 201, 102953.

Wang, Y., Cheng, H., Edwards, R.L., He, Y., Kong, X., An, Z., Wu, J., Kelly, M.J., Dykoski, C.A., Li, X., 2005. The Holocene Asian monsoon: links to solar changes and North Atlantic climate. Science 308, 854–857. https://doi.org/10.1126/science.1106296.

Yadava, A.K., Braeuning, A., Singh, J., Yadav, R.R., 2016. Boreal spring precipitation variability in the cold arid western Himalaya during the last millennium, regional linkages, and socio-economic implications. Quat. Sci. Rev. 144, 28–43. https://doi.org/10.1016/j.quascirev.2016.05.008.